

MoD-DPO: Towards Mitigating Cross-modal Hallucinations in Omni LLMs using Modality Decoupled Preference Optimization

Ashutosh Chaubey, Jiacheng Pang, Mohammad Soleymani
 Institute for Creative Technologies, University of Southern California
 achaubey@usc.edu, soleymani@ict.usc.edu

Project Page: mod-dpo.github.io

Abstract

Omni-modal large language models (omni LLMs) have recently achieved strong performance across audiovisual understanding tasks, yet they remain highly susceptible to cross-modal hallucinations arising from spurious correlations and dominant language priors. In this work, we propose Modality-Decoupled Direct Preference Optimization (MoD-DPO), a simple and effective framework for improving modality grounding in omni LLMs. MoD-DPO introduces modality-aware regularization terms that explicitly enforce invariance to corruptions in irrelevant modalities and sensitivity to perturbations in relevant modalities, thereby reducing unintended cross-modal interactions. To further mitigate over-reliance on textual priors, we incorporate a language-prior debiasing penalty that discourages hallucination-prone text-only responses. Extensive experiments across multiple audiovisual hallucination benchmarks demonstrate that MoD-DPO consistently improves perception accuracy and hallucination resistance, outperforming previous preference optimization baselines under similar training budgets. Our findings underscore the importance of modality-faithful alignment and demonstrate a scalable path toward more reliable and resilient multimodal foundation models.

1. Introduction

Recent progress in multimodal (or “omni”) large language models has rapidly expanded language-only reasoning into rich perceptual settings that span images, audio, and video [1, 9, 12, 43, 47]. Systems such as OmniVinci [47] demonstrate that carefully designed alignment modules, temporal representations, and curated omni-modal dialogue data can unlock strong cross-modal understanding at competitive efficiency. At the same time, foundation series like Qwen2.5 Omni [43] have shown that scale, post-training via DPO [31]/GRPO [34], and tool-augmented vocabularies translate into broadly useful capabilities and robust

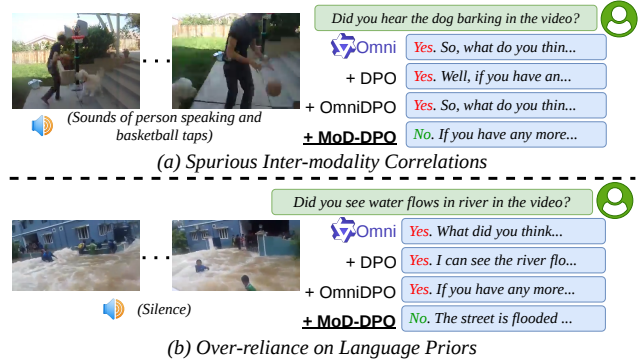


Figure 1. Comparison of the proposed MoD-DPO with other preference optimization baselines for mitigating cross-modal hallucinations arising from spurious inter-modality correlations and over-reliance on language priors.

instruction following across modalities. Beyond single-turn perception, emerging omni LLMs aim for unified, interactive audiovisual-language reasoning, pointing toward agents that both *see* and *listen* before they *think* and *respond* [36].

Despite impressive capabilities, state-of-the-art models are susceptible to *cross-modal hallucinations* (see Fig. 1) when audio and video provide subtle, asynchronous, or weakly correlated evidence [25, 35]. For example, hearing imaginary sounds from visual cues or perceiving non-existent visual events prompted by audio. Prior analyses [25] attribute these failures to (i) over-reliance on unimodal priors (especially language), and (ii) spurious inter-modality correlations learned during pretraining and alignment. Existing approaches begin to address these issues by explicitly training models to attend to evidence grounded in the correct modality [35] or using preference optimization with multimodal preference [4], but they neither *decouple* modality pathways during optimization nor penalize latent language-only shortcuts explicitly. In parallel, decoding-time defenses such as Visual Contrastive Decoding (VCD) [24] and its audiovisual extensions [21] can reduce hallucination without retraining, but they operate post hoc and do

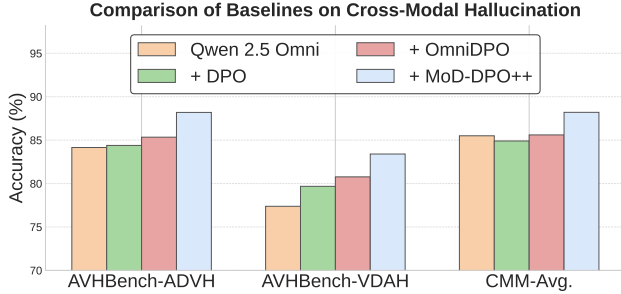


Figure 2. Comparison of proposed MoD-DPO++ with other preference optimization baselines on AVHBench [35] and CMM [25]. Average accuracy is reported. ADVH: Audio-driven video hallucination, VDAH: Video-driven audio hallucination.

not change the model’s internal decision boundaries.

To remove spurious inter-modality correlations and resulting cross-modal hallucinations, we propose a novel preference optimization technique that *explicitly decouples* modalities during training by enforcing two complementary properties: *invariance* to perturbations of irrelevant modalities and *sensitivity* to the corruption of the relevant modality to generate responses corresponding to prompts related to a modality. Our Modality-Decoupled DPO (MoD-DPO) formalizes these desiderata by adding KL-based regularizers to the original DPO objective [31] that (1) keep predictions stable when the unused (irrelevant) modality is corrupted and (2) amplify distributional shifts when the task-relevant modality is corrupted, yielding gradients that nudge the policy toward modality-faithful evidence use. Unlike prior works on multimodal DPO [4, 15, 37], we derive a closed-form solution to our MoD-DPO objective and optimize using an automatically generated preference dataset.

Since the LLM backbones in omni LLMs are pretrained on large-scale text data, they have strong language priors, which cause over-reliance on language inputs while neglecting audiovisual inputs. To mitigate this issue, we penalize the reward obtained for the closed-form optimal policy during preference optimization [31] to ensure that the model responses obtained only using the language inputs are suppressed.

We evaluate the proposed preference optimization technique on cross-modal hallucination benchmarks – AVH-Bench [35] and Curse of Multi-Modalities (CMM) [25] – and report a superior performance of the reference model compared to other post-training techniques as shown in Fig. 2. To summarize, the major contributions of our work are as follows.

- We propose MoD-DPO, a preference optimization technique to mitigate cross-modal hallucinations in omni LLMs. To support training, we construct a novel preference dataset with over 18.1k automatically generated samples spanning over 10.8k unique videos.
- To further reduce the effect of language model priors in

omni LLMs, we introduce a language prior debiasing penalty in the preference optimization reward.

- We perform experiments on multiple benchmarks to show the efficacy of the proposed approach in mitigating cross-modal hallucinations, outperforming other post-training methods.

2. Related Works

2.1. Multimodal Hallucination

Large multimodal models often generate content not grounded in the input. Recent works have proposed numerous benchmarks to expose cross-modal failures, in the context of vision-language [6, 13, 27, 52], audiovisual [35], and broad audiovisual-language hallucinations [25, 53]. Another detection technique leverages LLM cross-modal attention patterns to reveal traces of hallucination [54].

To alleviate vision-language hallucinations, two groups of methods have been extensively explored: training-time mitigation and decoding-time defenses. Training-time mitigation focuses on the creation of novel datasets [3, 14] and the introduction of new learning objectives that attempt to penalize ungrounded generation and reduce prior-induced hallucinations [16, 28, 48]. Decoding-time defenses include contrastive decoding techniques that reduce inconsistencies between logits and evidence, first observed in vision [24] and then in audiovisual settings [21]. Instruction-contrastive and adaptive focal-contrast methods [7] further reshape token probabilities at inference time. Visualization-assisted contrastive decoding and retrospective resampling promote self-consistency without retraining [30, 39]. Additionally, several works extended reinforcement learning from human feedback (RLHF) to multimodal LLMs for hallucination mitigation and human value alignment [20, 49, 55, 56].

2.2. Multimodal Policy Optimization

Direct Preference Optimization (DPO) offers a rollout-free alternative to RLHF and has been adapted to mitigate multimodal hallucinations [4, 15, 37]. Instead of costly human labels, many studies derive preference data from strong vision-language referee models, retrieval-augmented contexts, and synthetic preferences produced by reward models and LM-based evaluators [29, 38, 41, 45, 50]. Several formulations explicitly target hallucinations by skewing preference pairs toward grounded responses or by framing omni-modal mitigation within unified pipelines [4, 11]. However, vanilla multimodal DPO often fails to enforce modality-conditioned preferences, leaving models prone to language-prior shortcuts.

V-DPO [40] mitigates vision–language hallucinations by injecting video guidance into preference learning through a divergence term that discourages reliance on text-only

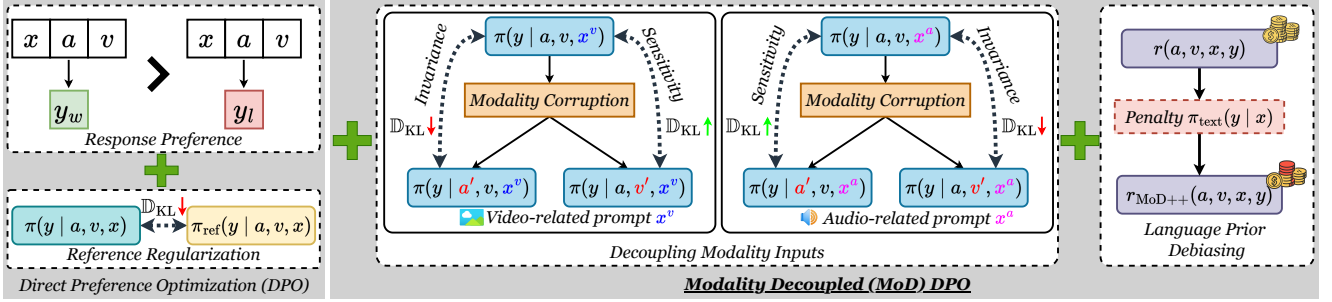


Figure 3. **Modality Decoupled Preference Optimization.** In addition to the response preference and reference regularization terms in DPO [31], we include additional KL regularization terms to increase model invariance to irrelevant modalities and model sensitivity to relevant modalities. Additionally, we penalize response generation with only text inputs to remove language priors in the model.

policies and uses image-contrast pairs to reinforce visual grounding; mDPO [37] strengthens multimodal conditioning via conditional preference terms comparing responses under informative versus degraded images and a reward anchor that prevents down-weighting correct answers; VistaDPO [15] extends preference optimization to videos using hierarchical preferences across instances, time, and regions; and OmniDPO [4] generalizes to audio–visual–language settings with text-preference and multimodal-preference pairs that promote attention to visual and auditory evidence. In contrast, our MoD-DPO method is objective-centric and modality-aware, enforcing invariance to perturbations in irrelevant modalities, sensitivity to corruptions in the relevant one, and incorporating a text-only debiasing penalty that directly counters dominant text priors driving multimodal hallucination.

3. Preliminary

Direct Preference Optimization (DPO) [31] aligns large language models (LLMs) with human preferences without the need for training a separate reward model. Given a reference language model π_{ref} , the standard reinforcement learning objective [19] for optimizing a policy π_{θ} is defined as:

$$\max_{\pi_{\theta}} \mathbb{E}_{x \sim \mathcal{D}, y \sim \pi_{\theta}(\cdot | x)} [r(x, y)] - \beta \mathbb{D}_{\text{KL}}(\pi_{\theta}(\cdot | x) \| \pi_{\text{ref}}(\cdot | x)), \quad (1)$$

where $r(x, y)$ is the reward assigned to response y for a given prompt x , β is a hyperparameter and $\mathbb{D}_{\text{KL}}(\cdot \| \cdot)$ denotes the Kullback–Leibler divergence [23]. This objective encourages the model to produce high-reward responses while ensuring that the learned policy π_{θ} remains close to the reference policy π_{ref} . The optimal policy for Eq. (1) yields the following reward function:

$$r(x, y) = \beta \frac{\log \pi(y | x)}{\log \pi_{\text{ref}}(y | x)} + \beta Z(x), \quad (2)$$

where $Z(x)$ is a partition function independent of both π_{θ} and y . Using the Bradley-Terry [2] model to model human

preferences results in the following loss function for DPO,

$$\mathcal{L}_{\text{DPO}} = -\mathbb{E} \left[\sigma \left(\beta \left(\log \frac{\pi_{\theta}(y_w | x)}{\pi_{\text{ref}}(y_w | x)} - \log \frac{\pi_{\theta}(y_l | x)}{\pi_{\text{ref}}(y_l | x)} \right) \right) \right] \quad (3)$$

where the expectation is over a preference dataset $\mathcal{D}_{\text{text}}^{\text{pref}} = \{(x, y_w, y_l)_i\}$ with y_w as the chosen response and y_l as the rejected response. $\sigma(\cdot)$ denotes the sigmoid function.

4. Modality Decoupled (MoD) DPO

Our goal is to mitigate *cross-modal hallucinations* in omni LLMs, which often arise from spurious inter-modal dependencies and over-relying on language model priors [25, 35]. To address this issue, we extend the DPO framework by modifying the original reinforcement learning objective in Eq. (1) to explicitly decouple modality-specific information in the model’s inputs, thereby reducing unwanted modality interactions.

For an omni LLM that processes both audio and visual inputs, the DPO objective can be generalized as,

$$\max_{\pi_{\theta}} \mathbb{E} [r(a, v, x, y)] - \beta \mathbb{D}_{\text{KL}}(\pi_{\theta}(\cdot | a, v, x) \| \pi_{\text{ref}}(\cdot | a, v, x)), \quad (4)$$

where a and v denote the audio and visual modalities, respectively, and the expectation is taken over an audiovisual dataset \mathcal{D}_{av} .

4.1. Decoupling Modality Inputs

We seek to decouple modality information by enforcing two key properties:

- (i) **Invariance:** The output distribution should remain stable when the *prompt-irrelevant* modality is corrupted, making the model response agnostic to changes in irrelevant input information.
- (ii) **Sensitivity:** The output distribution should shift appropriately when the *prompt-relevant* modality is corrupted, making the model response more sensitive to important input information.

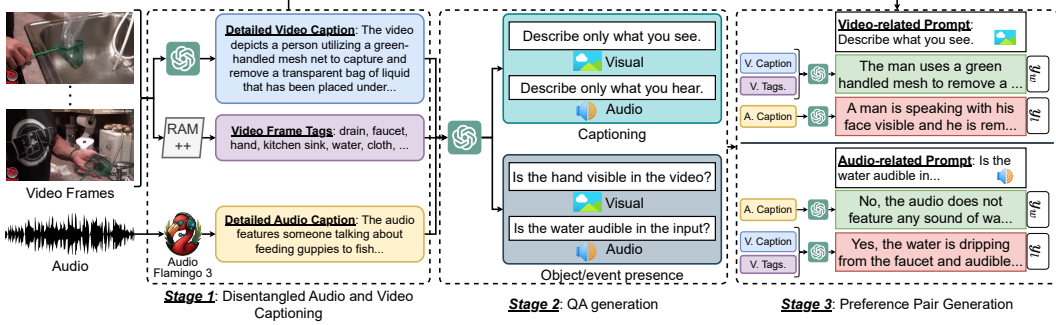


Figure 4. **Preference Data Generation Pipeline.** We disentangle the audiovisual input to obtain separate audio and visual captions or tags (Stage 1), which are then used to generate QA pairs for Stage 2. Finally, we create preference data for modality-specific questions by constructing chosen responses using relevant modality information and rejected responses using irrelevant modality information.

Specifically, let us assume that the input prompt x^v is related to the visual modality. Then our objective in Eq. (4) changes to the following,

$$\begin{aligned} \max_{\pi_{\theta}} \mathbb{E}_{(a,v,x^v) \sim \mathcal{D}, y \sim \pi_{\theta}(\cdot | a,v,x^v)} [r(a,v,x^v, y)] \\ - \beta \mathbb{D}_{\text{KL}}(\pi_{\theta}(\cdot | a,v,x^v) \| \pi_{\text{ref}}(\cdot | a,v,x^v)) \\ - \beta_{\text{inv}} \mathbb{D}_{\text{KL}}(\pi_{\theta}(\cdot | a,v,x^v) \| \pi_{\theta}(\cdot | a',v,x^v)) \\ + \beta_{\text{sens}} \mathbb{D}_{\text{KL}}(\pi_{\theta}(\cdot | a,v,x^v) \| \pi_{\theta}(\cdot | a,v',x^v)), \end{aligned} \quad (5)$$

where a' and v' denote corrupted versions of the audio and visual inputs, respectively. The green-highlighted term enforces *invariance* to corruption in the irrelevant modality (audio), while the blue-highlighted term enforces *sensitivity* to corruption in the relevant modality (visual). The hyperparameters β_{inv} and β_{sens} control the respective strengths of these regularization effects. Fig. 3 shows the comparison of the proposed approach with vanilla DPO.

The optimal policy π^* for Eq. (5) can be obtained using the method of Lagrange multipliers. However, unlike the standard DPO objective in Eq. (1), this modified formulation introduces additional dependencies on $\pi_{\theta}(y | a',v,x)$ and $\pi_{\theta}(y | a,v',x)$, which complicate the optimization process. To address this challenge, we assume these terms remain constant within each optimization step and treat them as fixed target distributions when computing the additional KL divergence terms in Eq. (5).

Under this assumption, we can take the partial derivative of Eq. (5) with respect to $\pi_{\theta}(y | a,v,x^v)$ and solve for the stationary point, yielding the following optimal policy,

$$\begin{aligned} \pi_{\theta}^*(y | a,v,x^v) \propto \exp(r(a,v,x^v, y)) \pi_{\text{ref}}(y | a,v,x^v)^{\beta/\tau} \\ \pi_{\theta}^*(y | a',v,x^v)^{\beta_{\text{inv}}/\tau} \pi_{\theta}^*(y | a,v',x^v)^{-\beta_{\text{sens}}/\tau}, \end{aligned} \quad (6)$$

where $\tau = \beta + \beta_{\text{inv}} + \beta_{\text{sens}}$, and π_{θ}^* denotes the fixed target distributions corresponding to corrupted audiovisual inputs. We detail the above proof in Supp. A.1.

Inspecting Eq. (6), we observe that the optimal policy increases the likelihood of correct responses when the ir-

relevant modality is corrupted (invariance) while penalizing the likelihood when the relevant modality is corrupted (sensitivity). This balance encourages the model to focus on modality-relevant cues while suppressing spurious cross-modal dependencies.

We can find the optimal reward function for Eq. (6) as the following,

$$\begin{aligned} r_{\text{MoD}}(a,v,x^v, y) = \tau \log \pi_{\theta}(y | a,v,x^v) - \beta \log \pi_{\text{ref}}(y | a,v,x^v) \\ - \beta_{\text{inv}} \log \pi_{\theta}'(y | a',v,x^v) + \beta_{\text{sens}} \log \pi_{\theta}'(y | a,v',x^v) \\ + W(a,v,x), \end{aligned} \quad (7)$$

where $W(a,v,x)$ is obtained by normalizing Eq. (6). Please refer to the Supp. A.2 & A.3 for more details. We can substitute this reward function into the Bradley-Terry model, similar to Eq. (3) to obtain the loss function for modality decoupled preference optimization as follows,

$$\begin{aligned} \mathcal{L}_{\text{MoD}}^v = -\mathbb{E} \left[\log \sigma \left(\tau \log \frac{\pi_{\theta}(y_w | a,v,x^v)}{\pi_{\theta}(y_l | a,v,x^v)} - \beta \log \frac{\pi_{\text{ref}}(y_w | a,v,x^v)}{\pi_{\text{ref}}(y_l | a,v,x^v)} \right. \right. \\ \left. \left. - \beta_{\text{inv}} \log \frac{\pi_{\theta}'(y_w | a',v,x^v)}{\pi_{\theta}'(y_l | a',v,x^v)} + \beta_{\text{sens}} \log \frac{\pi_{\theta}'(y_w | a,v',x^v)}{\pi_{\theta}'(y_l | a,v',x^v)} \right) \right], \end{aligned} \quad (8)$$

where $\tau = \beta + \beta_{\text{inv}} + \beta_{\text{sens}}$. Note that this objective is only for prompts related to the visual modality. We can write a similar form for prompts x^a related to the audio modality as $\mathcal{L}_{\text{MoD}}^a$ (Supp. A.4). The final loss function for decoupling modality inputs is as follows,

$$\mathcal{L}_{\text{MoD}} = \mathcal{L}_{\text{MoD}}^v + \mathcal{L}_{\text{MoD}}^a \quad (9)$$

Practical considerations. To ensure that π_{θ}' (in Eqs. (6) to (8)) is a fixed target during training for an iteration, we stop gradient computation and accumulation when passing the corrupt versions of audiovisual inputs (a' , v') to the model being trained. Moreover, during training, we alternate between training a batch of vision-related prompts x^v and audio-related prompts x^a rather than having a

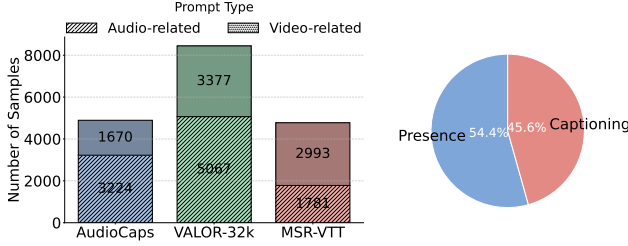


Figure 5. **Preference Data Statistics.** (Left) Number of preference samples generated from different source datasets. (Right) Composition of samples belonging to different tasks.

mixed batch. Additionally, we set β_{inv} lower than β_{sens} , as cross-modal information is sometimes beneficial even if the prompts are specific to a particular modality. For example, the presence of a visual entity (such as a dog) can be confirmed by its sound (barking) in the audio. Please see Sec. 6.2 (and Supp. D.1) for empirical analysis.

What about audiovisual inputs? We only perform DPO training on queries strongly linked to one of the modalities. We can modify the objective in Eq. (5) to get $\mathcal{L}_{\text{MoD}}^{av}$ for audiovisual tasks (like audiovisual captioning) as shown in Supp. A.5. However, our empirical results show that including such an objective during DPO training results in insignificant performance gains for eliminating cross-modal hallucinations (Sec. 6.2 and Tab. 6).

4.2. Language-Prior Debiasing (LPD)

To ensure that the language priors in the omni LLM do not solely control the outputs [25] (e.g., Fig. 1 - bottom), we introduce a language prior debiasing penalty to the preference optimization reward $r(a, v, x^v, y)$ in Eq. (7) to reduce the log-probability of the chosen response given just the text inputs x^v (Fig. 3). More concretely, our LPD penalty for a given input-response pair is as follows,

$$r_{\text{LPD}}(x^v, y) = -\log \pi_{\text{text}}(y | x^v), \quad (10)$$

where π_{text} is a language model which can take text-only inputs. Note that π_{text} is a frozen language model which captures language priors, and theoretically it can be any strong language model. However, we choose π_{text} as the reference model π_{ref} for efficiency. The total reward in Eq. (7) using this penalty becomes,

$$r_{\text{MoD++}}(a, v, x^v, y) = r_{\text{MoD}}(a, v, x^v, y) + \gamma_{\text{LPD}} r_{\text{LPD}}(x^v, y), \quad (11)$$

where γ_{LPD} is a hyperparameter to control language prior debiasing. The final objective (**MoD-DPO++**) with additional language prior debiasing becomes the following,

$$\mathcal{L}_{\text{MoD++}} = \mathcal{L}_{\text{MoD}} - \gamma_{\text{LPD}} \log \frac{\pi_{\text{ref}}(y_w | x)}{\pi_{\text{ref}}(y_l | x)}, \quad (12)$$

where x is a combined representation to denote prompts related to audio (x^a) and video (x^v).

Complexity Analysis. The proposed MoD-DPO++ framework introduces additional computational overhead per preference tuning iteration compared to standard DPO. Specifically, our objective requires additional forward passes for corrupted audio and visual inputs to enforce modality invariance and sensitivity. Moreover, the language prior debiasing (LPD) term involves an extra forward pass using text-only inputs. However, since none of the additional forward passes require gradient computation, additional gradient computation compared to Vanilla DPO is minimal. To maintain comparable training budgets, we therefore train MoD-DPO++ for only one quarter of the total epochs used by baseline methods. Please refer to Supp. A.6 for detailed analysis.

4.3. Training Dataset

Fig. 4 shows the preference data generation pipeline for performing the proposed preference optimization, comprising three stages. We ensure that the audiovisual information is decoupled during data generation to prevent the model from learning inter-modality spurious correlations. We summarize the stages of data generation in the following paragraphs with additional details present in Supp. B.1.

Stage 1. In the first stage, audio and visual inputs are separated and automatically annotated. For videos, we extract the visual captions through GPT-4o [18] and the visual tags through RAM++ [17, 51]. For audio, we extract the audio captions through AudioFlamingo 3 [12]. We source the original audiovisual files from MSR-VTT [42], VALOR32K (val) [5] and AudioCaps (val) [22]. In addition to the original audiovisual inputs with coupled audio and visual information, in most cases, we create mismatched audiovisual contexts using audio and video segments from different files, leading to improved performance (Sec. 6.2).

Stage 2. We automatically generate QA pairs using GPT-4o [18] for two tasks – audio/visual captioning and audio/visual object/event presence. These tasks are fundamental for audiovisual understanding, and as our results show, training on these tasks results in improvement in general audio and video tasks (Sec. 6.5) in addition to cross-modal hallucination benchmarks. Audio and visual information extracted in Stage 1 is provided to GPT-4o along with QA generation instructions.

Stage 3. Instead of generating rejected responses y_l which are completely irrelevant to an input prompt, we generate hard-negative rejected responses which include spurious information from the information extracted in the irrelevant modality. For example, to generate the rejected response for a prompt related to the visual modality, we create a rejected response by including information from the audio modality.

Table 1. Comparison of the proposed approach with other DPO and omni LLM methods on AVHBench [35].

| Method | Audio-driven Video Hallucination | | | | Video-driven Audio Hallucination | | | | Audiovisual Matching | | | |
|--------------------|----------------------------------|--------------|--------------|--------------|----------------------------------|--------------|--------------|--------------|----------------------|--------------|--------------|--------------|
| | Acc. | Pre. | Rec. | F1 | Acc. | Pre. | Rec. | F1 | Acc. | Pre. | Rec. | F1 |
| VideoLLaMA 2 [8] | 79.23 | 81.51 | 76.94 | 79.16 | 75.07 | 85.15 | 64.98 | 73.71 | 52.93 | 92.11 | 13.75 | 23.93 |
| VITA-1.5 [10] | 67.17 | 78.17 | 56.17 | 65.36 | 54.01 | 45.85 | 62.18 | 52.78 | 46.85 | 66.31 | 27.40 | 38.78 |
| OmniVinci [47] | 61.36 | 57.92 | 64.79 | 61.16 | 58.56 | 84.71 | 32.40 | 46.88 | 54.32 | 87.42 | 21.21 | 34.14 |
| Qwen 3 Omni [44] | 83.54 | 85.92 | 81.17 | 83.47 | 76.46 | 94.94 | 57.99 | 72.00 | 58.52 | 97.76 | 19.14 | 32.02 |
| Qwen 2.5 Omni [43] | 84.15 | 76.76 | 91.55 | 83.51 | 77.38 | 94.93 | 59.83 | 73.39 | 54.69 | 9.81 | 99.57 | 17.85 |
| + DPO [31] | 84.39 | 75.44 | 93.30 | 83.42 | 79.68 | 93.53 | 65.85 | 77.28 | 59.32 | 19.76 | 98.93 | 32.94 |
| + OmniDPO [4] | 85.34 | 75.61 | 95.06 | 84.23 | 80.77 | 86.36 | 75.19 | 80.39 | 61.50 | 23.90 | 99.14 | 38.52 |
| + MoD-DPO | 87.66 | 85.53 | 89.78 | 87.61 | 82.48 | 93.61 | 71.35 | 80.98 | 69.07 | 42.09 | 96.04 | 58.53 |
| + MoD-DPO++ | 88.19 | 86.35 | 90.02 | 88.15 | 83.40 | 93.82 | 72.98 | 82.10 | 69.68 | 43.32 | 96.04 | 59.71 |
| MiniCPM-O 2.6 [46] | 83.36 | 85.56 | 81.16 | 83.30 | 74.54 | 82.27 | 66.81 | 73.74 | 54.26 | 56.72 | 51.81 | 54.15 |
| + DPO [31] | 82.91 | 84.56 | 81.26 | 82.88 | 78.86 | 82.82 | 68.89 | 75.22 | 54.56 | 55.91 | 53.20 | 54.52 |
| + OmniDPO [4] | 84.96 | 86.18 | 83.75 | 84.95 | 75.39 | 80.56 | 70.22 | 75.04 | 56.86 | 57.82 | 55.90 | 56.84 |
| + MoD-DPO | 87.08 | 89.28 | 84.87 | 87.02 | 79.00 | 82.18 | 75.81 | 78.87 | 60.57 | 62.16 | 58.98 | 60.53 |
| + MoD-DPO++ | 87.26 | 88.89 | 85.63 | 87.23 | 79.49 | 82.39 | 76.58 | 79.38 | 60.66 | 61.87 | 59.45 | 60.64 |

Data Statistics. We generate a total of 18,112 preference data samples over 10,854 unique videos using the above pipeline. Fig. 5 shows the statistics of the preference dataset. Preference data samples are present in Supp. B.2.

5. Experimental Details

5.1. Evaluation Benchmarks and Metrics

Benchmarks. We evaluate our post-trained model for cross-modal hallucinations using AVHBench [35] and Curse of Multi-Modalities (CMM) Benchmark [25]. AVHBench tests cross-modal hallucination and audiovisual context matching with around 5k samples over 2k unique videos. CMM consists of tasks to test over-reliance on unimodal priors and spurious inter-modal correlations with 2.4k samples over 1.2k unique videos. For testing the general audio/visual capabilities of the model after DPO, we use DailyOmni [58] for joint audiovisual understanding, MVBench [26] for visual understanding, and MMAU [33] for audio understanding.

Evaluation Metrics. We report the accuracy, precision, recall, and F1 over the different tasks in AVHBench. For CMM [25], we report the perception accuracy (pa) and hallucination resistance (hr) over all the tasks. For general datasets, we report the average accuracy over different tasks of the dataset. Refer Supp. C.2 for more details.

5.2. Implementation Details

We modify the LLaMAFactory [57] codebase to implement the proposed method and to report results on the preference optimization baselines. We perform our experiments using two reference models – Qwen 2.5 Omni [43] (7B params) and MiniCPM-O 2.6 [46] (8B params). We train the proposed MoD-DPO with a learning rate of $3e^{-7}$ for a single epoch on the preference data using a batch size of 1 per GPU on 8 H100 GPUs. As discussed in Sec. 4.2, for a fair

comparison with MoD-DPO++, we train the baseline preference optimization techniques for four epochs. We choose $\beta = 0.1$ consistent with other DPO baselines [15, 37], where as $\beta_{\text{sens}} = 0.05$, $\beta_{\text{inv}} = 0.02$, and $\gamma_{\text{LPD}} = 0.05$ based on hyperparameter tuning (Sec. 6.2).

6. Results

6.1. Cross-Modal Hallucination Benchmarks

Tab. 1 shows the performance of the proposed approach on AVHBench [35] with comparison to several baselines. We can clearly see that MoD-DPO and MoD-DPO++ outperform all other baselines for overall accuracy and F1, showing a balanced performance. MoD-DPO results in gains of up to 27% accuracy relative to the reference models on the audiovisual matching task. On the CMM [25] Benchmark in Tab. 2, we can see similar trends with around 3-4 % overall performance gain over the reference models. Note that for the language dominance task, the improvement of MoD-DPO++ over MoD-DPO is significantly higher than in other tasks, thus showing the efficacy of LPD (Sec. 4.2) in reducing language priors.

6.2. Ablation Studies

Effect of different components. Tab. 3 shows the performance of Qwen 2.5 Omni [43] with MoD-DPO++ on AVHBench [35] and CMM [25] when different components of the proposed approach are ablated. We report the average metrics across different tasks within each benchmark. Sensitivity, Invariance and LPD are ablated by setting the corresponding hyperparameters β_{sens} , β_{inv} and γ_{LPD} to zero. Using LPD increases prediction recall and hallucination resistance significantly, showing that LPD significantly reduces language prior-induced hallucinations.

Choice of rejected and corrupt samples. Tab. 4 shows the performance variation with different forms of rejected

Table 2. Comparison of the proposed approach with other DPO and omni LLM methods on Curse of Multi-Modalities [25].

| Method | Spurious Inter-modality Correlation | | | | | | Uni-modality Over-reliance | | | | | | Overall | |
|--------------------|-------------------------------------|-------------|-------------|-------------|-------------|-------------|----------------------------|-------------|-------------|-------------|-------------|-------------|-------------|-------------|
| | VL | | AL | | VAL | | Visual Dom. | | Audio Dom. | | Lang. Dom. | | pa | hr |
| | pa | hr | pa | hr | pa | hr | pa | hr | pa | hr | pa | hr | | |
| VideoLLaMA 2 [8] | 75.0 | 86.0 | 77.5 | 94.0 | 78.0 | 98.0 | 62.0 | 75.5 | 80.0 | 90.0 | 57.5 | 43.0 | 71.7 | 81.1 |
| VITA 1.5 [10] | 92.5 | 91.5 | 42.5 | 30.5 | 77.7 | 72.9 | 57.0 | 24.4 | 77.4 | 67.7 | 86.0 | 55.5 | 72.2 | 57.1 |
| OmniVinci [47] | 88.5 | 81.0 | 74.5 | 90.0 | 98.0 | 72.0 | 91.0 | 63.5 | 96.0 | 35.0 | 87.0 | 75.0 | 89.2 | 69.4 |
| Qwen 3 Omni [44] | 96.5 | 77.5 | 93.0 | 88.0 | 97.5 | 94.0 | 95.5 | 60.0 | 94.5 | 67.0 | 93.0 | 65.0 | 95.0 | 75.3 |
| Qwen 2.5 Omni [43] | 88.0 | 98.0 | 89.9 | 84.4 | 93.0 | 93.5 | 87.8 | 67.7 | 85.3 | 80.7 | 74.2 | 83.2 | 86.4 | 84.6 |
| + DPO [31] | 86.0 | 98.5 | 89.5 | 86.5 | 92.4 | 94.4 | 86.7 | 63.5 | 84.3 | 80.4 | 72.5 | 84.1 | 85.2 | 84.6 |
| + OmniDPO [4] | 89.0 | 98.0 | 89.5 | 83.5 | 94.0 | 93.0 | 88.8 | 69.9 | 86.1 | 81.3 | 72.2 | 82.6 | 86.6 | 84.7 |
| + MoD-DPO | 91.5 | 98.5 | 92.3 | 83.2 | 94.5 | 94.5 | 92.3 | 74.2 | 88.4 | 83.8 | 73.9 | 83.1 | 88.8 | 86.2 |
| + MoD-DPO++ | 92.5 | 98.5 | 92.7 | 85.8 | 94.5 | 95.5 | 91.3 | 75.1 | 89.1 | 84.3 | 74.9 | 83.8 | 89.2 | 87.2 |
| MiniCPM-O 2.6 [46] | 87.0 | 94.0 | 90.5 | 74.0 | 87.0 | 84.0 | 79.5 | 80.5 | 87.4 | 76.4 | 82.0 | 73.7 | 85.6 | 80.4 |
| + DPO [31] | 87.0 | 93.0 | 89.5 | 74.5 | 86.0 | 84.5 | 79.5 | 79.5 | 87.8 | 76.0 | 81.5 | 74.3 | 85.2 | 80.3 |
| + OmniDPO [4] | 88.0 | 95.0 | 91.0 | 76.5 | 88.5 | 84.0 | 79.1 | 78.8 | 88.4 | 77.8 | 83.2 | 71.6 | 86.4 | 80.6 |
| + MoD-DPO | 90.5 | 95.5 | 92.0 | 76.0 | 91.5 | 86.0 | 82.5 | 84.8 | 89.0 | 78.9 | 82.4 | 73.7 | 88.0 | 82.5 |
| + MoD-DPO++ | 90.0 | 96.5 | 92.5 | 77.5 | 91.5 | 87.0 | 83.5 | 85.6 | 88.4 | 79.6 | 83.8 | 75.1 | 88.3 | 83.6 |

Table 3. Ablation study shows performance improvement of Qwen 2.5 Omni [43] using different components of the proposed MoD-DPO++. LPD: Language Prior Debiasing.

| Sens. | Inv. | LPD | AVHBench[35] | | | CMM[25] | |
|-------|------|-----|--------------|--------------|--------------|-------------|-------------|
| | | | Acc. | Pre. | Rec. | pa | hr |
| ✗ | ✗ | ✗ | 72.07 | 60.50 | 83.65 | 86.4 | 84.6 |
| ✓ | ✗ | ✗ | 77.02 | 69.82 | 84.21 | 87.4 | 85.1 |
| ✗ | ✓ | ✗ | 76.04 | 67.18 | 84.89 | 87.0 | 85.4 |
| ✓ | ✓ | ✗ | 79.74 | 73.74 | 85.72 | 88.8 | 86.2 |
| ✗ | ✗ | ✓ | 73.88 | 63.18 | 84.58 | 86.9 | 86.3 |
| ✓ | ✓ | ✓ | 80.42 | 74.50 | 86.34 | 89.2 | 87.2 |

Table 4. Performance comparison using different forms of rejected samples for MoD-DPO++ on Qwen 2.5 Omni [43]. y_i : rejected text response, a'/v' : corrupt audio/visual inputs, O: all zeros, RN: gaussian random noise, RAV: random audio/visual input, Diff.: diffusion-based corruption, t : steps for diffusion corruption.

| y_i | a'/v' | t | AVHBench [35] | | | CMM [25] | |
|------------|---------|-----|---------------|--------------|--------------|-------------|-------------|
| | | | Acc. | Pre. | Rec. | pa | hr |
| Rel. Opp. | O | - | 77.03 | 69.14 | 84.91 | 87.0 | 86.1 |
| Rel. Opp. | RN | - | 79.93 | 73.98 | 85.87 | 88.8 | 87.3 |
| Rel. Opp. | RAV | - | 79.03 | 71.87 | 86.18 | 88.4 | 86.3 |
| Rel. Opp. | Diff. | 10 | 72.72 | 62.16 | 83.28 | 86.3 | 84.9 |
| Rel. Opp. | Diff. | 50 | 76.92 | 69.52 | 84.32 | 87.1 | 85.4 |
| Rel. Opp. | Diff. | 500 | 80.42 | 74.50 | 86.34 | 89.2 | 87.2 |
| Irrelevant | Diff. | 500 | 77.91 | 71.18 | 84.64 | 88.1 | 85.4 |

(corrupt) samples for MoD-DPO. First, comparing the last two rows in Tab. 4, we can observe that using a rejected response relevant to the opposite modality as y_i leads to significant performance improvement compared to using a completely irrelevant response. We also report the performance of choosing different ways of corrupting audiovisual inputs in the first six rows of Tab. 4. We can observe that diffusing the inputs with noise (similar to VCD [24]) results in the best performance. Using a random video/audio and random noise also yields decent performance for the proposed approach. Additionally, using diffusion with a

smaller number of steps results in poor performance, as the corrupted inputs appear similar to the original inputs in this case, thereby spuriously shifting the KL divergence in the MoD-DPO loss.

Strength of hyperparameters. Supp. D.1 shows the effect of varying hyperparameters involved in MoD-DPO++. Increasing β_{sens} up to 0.1 leads to an increase in precision and perception accuracy in AVHBench and CMM, respectively; however, recall and hallucination resistance start dropping sharply after 0.1. For higher strengths of β_{inv} (> 0.02), model performance deteriorates significantly, which is consistent with the argument in the practical considerations in Sec. 4.1. Additionally, higher strengths of γ_{LPD} result in a sharp decline of precision and perception accuracy, as a heavy penalty on language priors even suppresses the desirable language priors in the backbone LLM.

Importance of using mismatched contexts. Tab. 6 illustrates the importance of using a combination of matched and mismatched audiovisual contexts in the training data proposed in Sec. 4.3. Matched context samples contain audio and video from the same source file, while mismatched ones use audio and video from different files. We can observe that using a mix of matched and mismatched audiovisual context results in superior performance.

Adding joint audiovisual data for preference training. We include an additional loss function for joint audiovisual tasks as described in Supp. A.5 to train on joint audiovisual tasks. We include tasks of audiovisual captioning and audiovisual matching in the preference dataset for this training. Tab. 6 (last row) shows the results of including audiovisual tasks, which do not result in significant improvement over the objective with just audio and visual tasks.

6.3. Robustness to Adversarial Inputs

Our MoD-DPO++ objective ensures that the output distribution remains robust to changes in the prompt-irrelevant

| Model | DailyOmni [58] | | | MVBench [26] | MMAU [33] | | | |
|--------------------|----------------|--------------|--------------|--------------|--------------|--------------|--------------|--------------|
| | 30s | 60s | Avg. | Avg. | Sound | Music | Speech | Avg. |
| Qwen 2.5 Omni [43] | 46.74 | 48.46 | 47.34 | 69.61 | 66.19 | 68.34 | 59.32 | 64.62 |
| + DPO [31] | 50.95 | 51.93 | 51.44 | 68.21 | 67.23 | 69.99 | 58.34 | 65.19 |
| + OmniDPO [4] | 49.24 | 50.89 | 50.07 | 68.89 | 67.58 | 69.87 | 59.11 | 65.52 |
| + MoD-DPO | 52.45 | 53.54 | 53.00 | 70.95 | 68.21 | 70.12 | 58.98 | 65.77 |
| + MoD-DPO++ | 53.45 | 54.18 | 53.82 | 71.02 | 68.16 | 71.60 | 59.24 | 66.33 |
| MiniCPM-O 2.6 [46] | 38.02 | 23.09 | 30.55 | 62.56 | 69.23 | 66.76 | 64.26 | 66.75 |
| + DPO [31] | 39.97 | 28.28 | 34.13 | 63.18 | 69.38 | 67.13 | 64.23 | 66.91 |
| + OmniDPO [4] | 40.68 | 27.98 | 34.33 | 64.42 | 70.65 | 69.15 | 63.38 | 67.73 |
| + MoD-DPO | 42.86 | 28.56 | 35.71 | 64.15 | 72.08 | 70.08 | 64.78 | 68.98 |
| + MoD-DPO++ | 43.33 | 29.87 | 36.60 | 64.32 | 71.34 | 69.23 | 64.91 | 68.30 |

Table 5. Comparison of the proposed approach with other DPO methods on general benchmarks: DailyOmni (audiovisual), MVBench (video), and MMAU (audio).

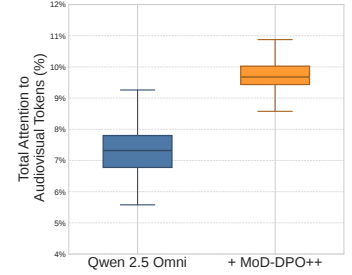


Figure 6. Total attention to audiovisual tokens as a percentage of total attention to input tokens (including text) on CMM [25].

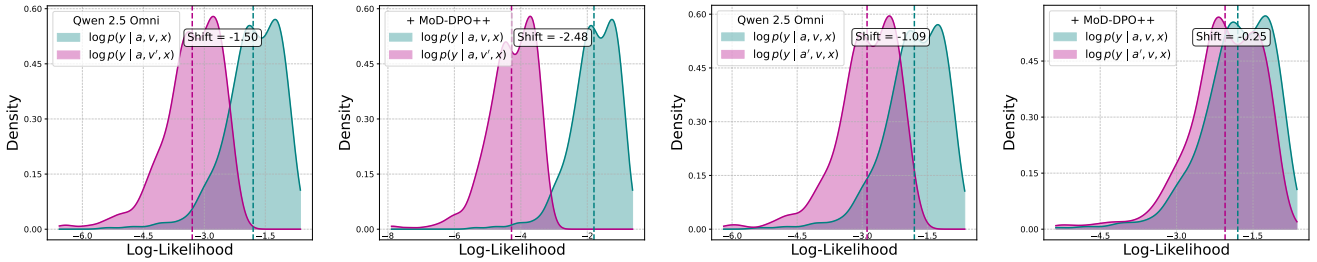


Figure 7. Distribution shift for the log-likelihood of the correct answer when the relevant modality is corrupted (*left two plots*) and when the irrelevant modality is corrupted (*right two plots*) for the audio-driven visual hallucination task in AVHBench [35]. MoD-DPO++ results in a larger shift when the relevant modality is corrupted (*sensitivity*) and lower shift when the irrelevant modality is corrupted (*invariance*).

Table 6. Effect of training with matched/mismatched audiovisual contexts and tasks in the preference training data. Reference is Qwen 2.5 Omni [43]. A: Audio-related, V: Video-related, AV: Joint audiovisual tasks.

| AV Context | Tasks | AVHBench[35] | | | CMM[25] | |
|------------|--------|--------------|--------------|--------------|-------------|-------------|
| | | Acc. | Pre. | Rec. | pa | hr |
| Mat. | A,V | 76.69 | 69.29 | 84.09 | 87.6 | 85.8 |
| Mis. | A,V | 78.24 | 72.18 | 84.29 | 88.2 | 86.1 |
| Mat.+Mis. | A,V | 80.42 | 74.50 | 86.34 | 89.2 | 87.2 |
| Mat.+Mis. | A,V,AV | 80.33 | 74.68 | 85.98 | 89.0 | 87.5 |

modality (*invariance*), while remaining sensitive to corruptions in the relevant modality. Fig. 7 shows the log-likelihood shifts (using Kernel Density Estimation) for the audio-driven video hallucination task in AVHBench [35] when the relevant (i.e., video) and irrelevant (i.e., audio) modalities of the input are corrupted. We can observe that the MoD-DPO++ is more invariant (robust) to corruptions in the irrelevant modality and is more sensitive to the corruptions in the relevant modality.

6.4. Attention Redistribution to Audiovisual Tokens

To show the efficacy of LPD (Sec. 4.2), we plot the distribution of combined audiovisual attention as a percent of the total attention to input tokens in generating responses for CMM [25] for both Qwen 2.5 Omni [43] and MoD-DPO++ trained models in Fig. 6. We take the average over all attention heads and all layers. We can see that with MoD-

DPO++, the total attention towards audiovisual tokens increases significantly, indicating that MoD-DPO++ forces the model to focus more on audiovisual inputs.

6.5. Performance on General Benchmarks

Tab. 5 shows the improvement in performance of Qwen 2.5 Omni [43] and MiniCPM-O 2.6 [46] on general benchmarks. We can see that while the baselines provide inconsistent performance gains, MoD-DPO++ provides consistent gains over all the benchmarks. Additionally, comparison with decode-time approaches is present in Supp. D.2 and multi-turn results are present in Supp. D.3.

7. Conclusion

We presented MoD-DPO, a modality-decoupled preference optimization framework designed to mitigate cross-modal hallucinations in omni LLMs. By enforcing invariance to irrelevant modality corruption and sensitivity to perturbations in the task-relevant modality, our method encourages models to ground their predictions in the appropriate evidence. Coupled with a language-prior debiasing penalty and a large automatically generated preference dataset, MoD-DPO consistently improves robustness across challenging audiovisual hallucination benchmarks. Our results highlight the importance of modality-faithful alignment and demonstrate that structured preference optimization is an effective direction for building reliable multimodal systems.

Acknowledgements

Research was sponsored by the Army Research Office and was accomplished under Cooperative Agreement Number W911NF-25-2-0040. The views and conclusions contained in this document are those of the authors and should not be interpreted as representing the official policies, either expressed or implied, of the Army Research Office or the U.S. Government. The U.S. Government is authorized to reproduce and distribute reprints for Government purposes notwithstanding any copyright notation herein.

References

- [1] Shuai Bai, Keqin Chen, Xuejing Liu, Jialin Wang, Wenbin Ge, Sibao Song, Kai Dang, Peng Wang, Shijie Wang, Jun Tang, Humen Zhong, Yuanzhi Zhu, Mingkun Yang, Zhaohai Li, Jianqiang Wan, Pengfei Wang, Wei Ding, Zheren Fu, Yiheng Xu, Jiabo Ye, Xi Zhang, Tianbao Xie, Zesen Cheng, Hang Zhang, Zhibo Yang, Haiyang Xu, and Junyang Lin. Qwen2.5-vl technical report. *arXiv preprint arXiv:2502.13923*, 2025. 1
- [2] Ralph Allan Bradley and Milton E. Terry. Rank analysis of incomplete block designs: I. the method of paired comparisons. *Biometrika*, 39(3/4):324, 1952. 3
- [3] Cong Chen, Mingyu Liu, Chenchen Jing, Yizhou Zhou, Fengyun Rao, Hao Chen, Bo Zhang, and Chunhua Shen. Perturbollava: Reducing multimodal hallucinations with perturbative visual training, 2025. 2
- [4] Junzhe Chen, Tianshu Zhang, Shiyu Huang, Yuwei Niu, Chao Sun, Rongzhou Zhang, Guanyu Zhou, Lijie Wen, and Xuming Hu. Omnidpo: A preference optimization framework to address omni-modal hallucination, 2025. 1, 2, 3, 6, 7, 8, 5
- [5] Sihan Chen, Xingjian He, Longteng Guo, Xinxin Zhu, Weining Wang, Jinhui Tang, and Jing Liu. Valor: Vision-audio-language omni-perception pretraining model and dataset. *arXiv preprint arXiv:2304.08345*, 2023. 5
- [6] Xiang Chen, Chenxi Wang, Yida Xue, Ningyu Zhang, Xiaoyan Yang, Qiang Li, Yue Shen, Lei Liang, Jinjie Gu, and Huajun Chen. Unified hallucination detection for multimodal large language models, 2024. 2
- [7] Zhaorun Chen, Zhuokai Zhao, Hongyin Luo, Huaxiu Yao, Bo Li, and Jiawei Zhou. Halc: Object hallucination reduction via adaptive focal-contrast decoding, 2024. 2
- [8] Zesen Cheng, Sicong Leng, Hang Zhang, Yifei Xin, Xin Li, Guanzheng Chen, Yongxin Zhu, Wenqi Zhang, Ziyang Luo, Deli Zhao, et al. Videollama 2: Advancing spatial-temporal modeling and audio understanding in video-llms. *arXiv preprint arXiv:2406.07476*, 2024. 6, 7, 5
- [9] Kaituo Feng, Kaixiong Gong, Bohao Li, Zonghao Guo, Yibing Wang, Tianshuo Peng, Junfei Wu, Xiaoying Zhang, Benyou Wang, and Xiangyu Yue. Video-rl: Reinforcing video reasoning in MLLMs. In *The Thirty-ninth Annual Conference on Neural Information Processing Systems*, 2025. 1
- [10] Chaoyou Fu, Haojia Lin, Xiong Wang, Yi-Fan Zhang, Yunhang Shen, Xiaoyu Liu, Yangze Li, Zuwei Long, Heting Gao, Ke Li, et al. Vita-1.5: Towards gpt-4o level real-time vision and speech interaction. *arXiv preprint arXiv:2501.01957*, 2025. 6, 7, 5
- [11] Yuhan Fu, Ruobing Xie, Xingwu Sun, Zhanhui Kang, and Xirong Li. Mitigating hallucination in multimodal large language model via hallucination-targeted direct preference optimization, 2024. 2
- [12] Sreyan Ghosh, Arushi Goel, Jaehyeon Kim, Sonal Kumar, Zhifeng Kong, Sang gil Lee, Chao-Han Huck Yang, Ramani Duraiswami, Dinesh Manocha, Rafael Valle, and Bryan Catanzaro. Audio flamingo 3: Advancing audio intelligence with fully open large audio language models. In *The Thirty-ninth Annual Conference on Neural Information Processing Systems*, 2025. 1, 5, 3, 7
- [13] Tianrui Guan, Fuxiao Liu, Xiyang Wu, Ruiqi Xian, Zongxia Li, Xiaoyu Liu, Xijun Wang, Lichang Chen, Furong Huang, Yaser Yacoub, Dinesh Manocha, and Tianyi Zhou. Hallusionbench: An advanced diagnostic suite for entangled language hallucination and visual illusion in large vision-language models, 2024. 2
- [14] Anisha Gunjal, Jihan Yin, and Erhan Bas. Detecting and preventing hallucinations in large vision language models, 2024. 2
- [15] Haojian Huang, Haodong Chen, Shengqiong Wu, Meng Luo, Jinlan Fu, Xinya Du, Hanwang Zhang, and Hao Fei. \mathcal{V} ista \mathcal{DPO} : Video hierarchical spatial-temporal direct preference optimization for large video models. In *Forty-second International Conference on Machine Learning*, 2025. 2, 3, 6
- [16] Qidong Huang, Xiaoyi Dong, Pan Zhang, Bin Wang, Conghui He, Jiaqi Wang, Dahua Lin, Weiming Zhang, and Nenghai Yu. Opera: Alleviating hallucination in multimodal large language models via over-trust penalty and retrospection-allocation, 2024. 2
- [17] Xinyu Huang, Yi-Jie Huang, Youcai Zhang, Weiwei Tian, Rui Feng, Yuejie Zhang, Yanchun Xie, Yaqian Li, and Lei Zhang. Open-set image tagging with multi-grained text supervision. In *Proceedings of the 33rd ACM International Conference on Multimedia*, pages 4117–4126, 2025. 5, 3
- [18] Aaron Hurst, Adam Lerer, Adam P Goucher, Adam Perelman, Aditya Ramesh, Aidan Clark, AJ Ostrow, Akila Welihinda, Alan Hayes, Alec Radford, et al. Gpt-4o system card. *arXiv preprint arXiv:2410.21276*, 2024. 5, 3, 7
- [19] Natasha Jaques, Judy Hanwen Shen, Asma Ghandeharioun, Craig Ferguson, Agata Lapedriza, Noah Jones, Shixiang Gu, and Rosalind Picard. Human-centric dialog training via offline reinforcement learning. In *Proceedings of the 2020 Conference on Empirical Methods in Natural Language Processing (EMNLP)*, pages 3985–4003, 2020. 3
- [20] Jiaming Ji, Jiayi Zhou, Hantao Lou, Boyuan Chen, Donghai Hong, Xuyao Wang, Wenqi Chen, Kaile Wang, Rui Pan, Jiahao Li, Mohan Wang, Josef Dai, Tianyi Qiu, Hua Xu, Dong Li, Weipeng Chen, Jun Song, Bo Zheng, and Yaodong Yang. Align anything: Training all-modality models to follow instructions with language feedback, 2024. 2

- [21] Chaeyoung Jung, Youngjoon Jang, and Joon Son Chung. AVCD: Mitigating hallucinations in audio-visual large language models through contrastive decoding. In *The Thirty-ninth Annual Conference on Neural Information Processing Systems*, 2025. 1, 2, 5
- [22] Chris Dongjoo Kim, Byeongchang Kim, Hyunmin Lee, and Gunhee Kim. AudioCaps: Generating captions for audios in the wild. In *Proceedings of the 2019 Conference of the North American Chapter of the Association for Computational Linguistics: Human Language Technologies, Volume 1 (Long and Short Papers)*, pages 119–132, Minneapolis, Minnesota, 2019. Association for Computational Linguistics. 5
- [23] S. Kullback and R. A. Leibler. On information and sufficiency. *The Annals of Mathematical Statistics*, 22(1):79–86, 1951. 3
- [24] Sicong Leng, Hang Zhang, Guanzheng Chen, Xin Li, Shijian Lu, Chunyan Miao, and Lidong Bing. Mitigating object hallucinations in large vision-language models through visual contrastive decoding. In *Proceedings of the IEEE/CVF Conference on Computer Vision and Pattern Recognition*, pages 13872–13882, 2024. 1, 2, 7
- [25] Sicong Leng, Yun Xing, Zesen Cheng, Yang Zhou, Hang Zhang, Xin Li, Deli Zhao, Shijian Lu, Chunyan Miao, and Lidong Bing. The curse of multi-modalities: Evaluating hallucinations of large multimodal models across language, visual, and audio. In *The Thirty-ninth Annual Conference on Neural Information Processing Systems Datasets and Benchmarks Track*, 2025. 1, 2, 3, 5, 6, 7, 8
- [26] Kunchang Li, Yali Wang, Yinan He, Yizhuo Li, Yi Wang, Yi Liu, Zun Wang, Jilan Xu, Guo Chen, Ping Luo, et al. Mvbench: A comprehensive multi-modal video understanding benchmark. In *Proceedings of the IEEE/CVF Conference on Computer Vision and Pattern Recognition*, pages 22195–22206, 2024. 6, 8, 5
- [27] Yifan Li, Yifan Du, Kun Zhou, Jimpeng Wang, Wayne Xin Zhao, and Ji-Rong Wen. Evaluating object hallucination in large vision-language models, 2023. 2
- [28] Xinyu Lyu, Beita Chen, Lianli Gao, Jingkuan Song, and Heng Tao Shen. Alleviating hallucinations in large vision-language models through hallucination-induced optimization, 2025. 2
- [29] Yassine Ouali, Adrian Bulat, Brais Martinez, and Georgios Tzimiropoulos. Clip-dpo: Vision-language models as a source of preference for fixing hallucinations in vlms, 2024. 2
- [30] Yeji Park, Deokyeong Lee, Junsuk Choe, and Buru Chang. Convis: Contrastive decoding with hallucination visualization for mitigating hallucinations in multimodal large language models, 2024. 2
- [31] Rafael Rafailov, Archit Sharma, Eric Mitchell, Christopher D Manning, Stefano Ermon, and Chelsea Finn. Direct preference optimization: Your language model is secretly a reward model. In *Thirty-seventh Conference on Neural Information Processing Systems*, 2023. 1, 2, 3, 6, 7, 8, 5
- [32] Anton Razzhigaev, Maxim Kurkin, Elizaveta Goncharova, Irina Abdullaeva, Anastasia Lysenko, Alexander Panchenko, Andrey Kuznetsov, and Denis Dimitrov. OmniDialog: A multimodal benchmark for generalization across text, visual, and audio modalities. In *Proceedings of the 2nd GenBench Workshop on Generalisation (Benchmarking) in NLP*, pages 183–195, Miami, Florida, USA, 2024. Association for Computational Linguistics. 6
- [33] S Sakshi, Utkarsh Tyagi, Sonal Kumar, Ashish Seth, Rameshwaran Selvakumar, Oriol Nieto, Ramani Duraiswami, Sreyan Ghosh, and Dinesh Manocha. MMAU: A massive multi-task audio understanding and reasoning benchmark. In *The Thirteenth International Conference on Learning Representations*, 2025. 6, 8, 5
- [34] Zhihong Shao, Peiyi Wang, Qihao Zhu, Runxin Xu, Junxiao Song, Xiao Bi, Haowei Zhang, Mingchuan Zhang, YK Li, et al. Deepseekmath: Pushing the limits of mathematical reasoning in open language models. *arXiv preprint arXiv:2402.03300*, 2024. 1
- [35] Kim Sung-Bin, Oh Hyun-Bin, Jungmok Lee, Arda Senocak, Joon Son Chung, and Tae-Hyun Oh. AVHBench: A cross-modal hallucination benchmark for audio-visual large language models. In *The Thirteenth International Conference on Learning Representations*, 2025. 1, 2, 3, 6, 7, 8, 4, 5
- [36] Wenwen Tong, Hewei Guo, Dongchuan Ran, Jiangnan Chen, Jiefan Lu, Kaibin Wang, Keqiang Li, Xiaoxu Zhu, Jiakui Li, Kehan Li, et al. Interactiveomni: A unified omni-modal model for audio-visual multi-turn dialogue. *arXiv preprint arXiv:2510.13747*, 2025. 1
- [37] Fei Wang, Wenxuan Zhou, James Y. Huang, Nan Xu, Sheng Zhang, Hoifung Poon, and Muhao Chen. mDPO: Conditional preference optimization for multimodal large language models. In *Proceedings of the 2024 Conference on Empirical Methods in Natural Language Processing*, pages 8078–8088, Miami, Florida, USA, 2024. Association for Computational Linguistics. 2, 3, 6
- [38] Robert Wijaya, Ngoc-Bao Nguyen, and Ngai-Man Cheung. Multimodal preference data synthetic alignment with reward model, 2024. 2
- [39] Tsung-Han Wu, Heekyung Lee, Jiaxin Ge, Joseph E. Gonzalez, Trevor Darrell, and David M. Chan. Generate, but verify: Reducing hallucination in vision-language models with retrospective resampling, 2025. 2
- [40] Yuxi Xie, Guanzhen Li, Xiao Xu, and Min-Yen Kan. V-dpo: Mitigating hallucination in large vision language models via vision-guided direct preference optimization, 2024. 2
- [41] Shuo Xing, Peiran Li, Yuping Wang, Ruizheng Bai, Yueqi Wang, Chan-Wei Hu, Chengxuan Qian, Huaxiu Yao, and Zhengzhong Tu. Re-align: Aligning vision language models via retrieval-augmented direct preference optimization, 2025. 2
- [42] Jun Xu, Tao Mei, Ting Yao, and Yong Rui. Msr-vtt: A large video description dataset for bridging video and language. In *Proceedings of the IEEE conference on computer vision and pattern recognition*, pages 5288–5296, 2016. 5
- [43] Jin Xu, Zhifang Guo, Jinzheng He, Hangrui Hu, Ting He, Shuai Bai, Keqin Chen, Jialin Wang, Yang Fan, Kai Dang, Bin Zhang, Xiong Wang, Yunfei Chu, and Junyang Lin. Qwen2.5-omni technical report, 2025. 1, 6, 7, 8, 5
- [44] Jin Xu, Zhifang Guo, Hangrui Hu, Yunfei Chu, Xiong Wang, Jinzheng He, Yuxuan Wang, Xian Shi, Ting He, Xinfan

- Zhu, et al. Qwen3-omni technical report. *arXiv preprint arXiv:2509.17765*, 2025. 6, 7, 5
- [45] Zhihe Yang, Xufang Luo, Dongqi Han, Yunjian Xu, and Dongsheng Li. Mitigating hallucinations in large vision-language models via dpo: On-policy data hold the key, 2025. 2
- [46] Yuan Yao, Tianyu Yu, Ao Zhang, Chongyi Wang, Junbo Cui, Hongji Zhu, Tianchi Cai, Haoyu Li, Weilin Zhao, Zhihui He, et al. Minicpm-v: A gpt-4v level mllm on your phone. *arXiv preprint arXiv:2408.01800*, 2024. 6, 7, 8
- [47] Hanrong Ye, Chao-Han Huck Yang, Arushi Goel, Wei Huang, Ligeng Zhu, Yuanhang Su, Sean Lin, An-Chieh Cheng, Zhen Wan, Jinchuan Tian, Yuming Lou, Dong Yang, Zhijian Liu, Yukang Chen, Ambrish Dantrey, Ehsan Jahangiri, Sreyan Ghosh, Daguang Xu, Ehsan Hosseini-Asl, Danial Mohseni Taheri, Vidya Murali, Sifei Liu, Jason Lu, Oluwatobi Olabiyi, Frank Wang, Rafael Valle, Bryan Catanzaro, Andrew Tao, Song Han, Jan Kautz, Hongxu Yin, and Pavlo Molchanov. Omnivinci: Enhancing architecture and data for omni-modal understanding llms. *arXiv preprint arXiv:2510.15870*, 2025. 1, 6, 7, 5
- [48] Shukang Yin, Chaoyou Fu, Sirui Zhao, Tong Xu, Hao Wang, Dianbo Sui, Yunhang Shen, Ke Li, Xing Sun, and Enhong Chen. Woodpecker: hallucination correction for multimodal large language models. *Science China Information Sciences*, 67(12), 2024. 2
- [49] Tianyu Yu, Yuan Yao, Haoye Zhang, Taiwen He, Yifeng Han, Ganqu Cui, Jinyi Hu, Zhiyuan Liu, Hai-Tao Zheng, Maosong Sun, and Tat-Seng Chua. Rlhf-v: Towards trustworthy mllms via behavior alignment from fine-grained correctional human feedback, 2024. 2
- [50] Ruohong Zhang, Liangke Gui, Zhiqing Sun, Yihao Feng, Keyang Xu, Yuanhan Zhang, Di Fu, Chunyuan Li, Alexander Hauptmann, Yonatan Bisk, and Yiming Yang. Direct preference optimization of video large multimodal models from language model reward, 2024. 2
- [51] Youcai Zhang, Xinyu Huang, Jinyu Ma, Zhaoyang Li, Zhaochuan Luo, Yanchun Xie, Yuzhuo Qin, Tong Luo, Yaqian Li, Shilong Liu, et al. Recognize anything: A strong image tagging model. In *Proceedings of the IEEE/CVF Conference on Computer Vision and Pattern Recognition*, pages 1724–1732, 2024. 5
- [52] Yongheng Zhang, Xu Liu, Ruoxi Zhou, Qiguang Chen, Hao Fei, Wenpeng Lu, and Libo Qin. Cchallenge: A novel benchmark for joint cross-lingual and cross-modal hallucinations detection in large language models, 2025. 2
- [53] Yiman Zhang, Ziheng Luo, Qiangyu Yan, Wei He, Borui Jiang, Xinghao Chen, and Kai Han. Omnieval: A benchmark for evaluating omni-modal models with visual, auditory, and textual inputs, 2025. 2
- [54] Yudong Zhang, Ruobing Xie, Xingwu Sun, Yiqing Huang, Jiansheng Chen, Zhanhui Kang, Di Wang, and Yu Wang. Dhcp: Detecting hallucinations by cross-modal attention pattern in large vision-language models, 2025. 2
- [55] Yi-Fan Zhang, Tao Yu, Haochen Tian, Chaoyou Fu, Peiyan Li, Jianshu Zeng, Wulin Xie, Yang Shi, Huanyu Zhang, Junkang Wu, Xue Wang, Yibo Hu, Bin Wen, Fan Yang, Zhang Zhang, Tingting Gao, Di Zhang, Liang Wang, Rong Jin, and Tieniu Tan. Mm-rlhf: The next step forward in multimodal llm alignment, 2025. 2
- [56] Xiangyu Zhao, Shengyuan Ding, Zicheng Zhang, Haian Huang, Maosong Cao, Weiyun Wang, Jiaqi Wang, Xinyu Fang, Wenhai Wang, Guangtao Zhai, Haodong Duan, Hua Yang, and Kai Chen. Omnialign-v: Towards enhanced alignment of mllms with human preference, 2025. 2
- [57] Yaowei Zheng, Richong Zhang, Junhao Zhang, Yanhan Ye, Zheyuan Luo, Zhangchi Feng, and Yongqiang Ma. Llamafactory: Unified efficient fine-tuning of 100+ language models. In *Proceedings of the 62nd Annual Meeting of the Association for Computational Linguistics (Volume 3: System Demonstrations)*, Bangkok, Thailand, 2024. Association for Computational Linguistics. 6
- [58] Ziwei Zhou, Rui Wang, and Zuxuan Wu. Daily-omni: Towards audio-visual reasoning with temporal alignment across modalities. *arXiv preprint arXiv:2505.17862*, 2025. 6, 8, 5

MoD-DPO: Towards Mitigating Cross-modal Hallucinations in Omni LLMs using Modality Decoupled Preference Optimization

Supplementary Material

Table of Contents

- Methodological Details Supp. A
 - Finding the Optimal Policy Supp. A.1
 - Reward Function for Optimal Policy Supp. A.2
 - Decoupled Loss Function Supp. A.3
 - Symmetric Objective for Audio-Related Prompts Supp. A.4
 - (Optional) Objective for Prompts requiring both audio and visual information Supp. A.5
 - Training compute details Supp. A.6
- Preference Data Details Supp. B
 - Detailed Pipeline Supp. B.1
 - Preference Data Samples Supp. B.2
- Experimental Details Supp. C
 - Evaluation Metrics Supp. C.1
 - Evaluation Protocol Supp. C.2
 - Baseline Implementations Supp. C.3
- Additional Results Supp. D
 - Hyper-parameter Tuning Supp. D.1
 - Comparison with decode-time approaches Supp. D.2
 - Multi-turn omni-modal results Supp. D.3
- Prompt Pool Supp. E

A. Methodological Details

A.1. Finding the Optimal Policy

Consider the objective in Eq. (5) for prompts that are related to the visual modality. For clarity, define $p_\theta \triangleq \pi_\theta(y \mid a, v, x^v)$, $p_{\text{ref}} \triangleq \pi_{\text{ref}}(y \mid a, v, x^v)$, $q_{\text{inv}}(y) \triangleq \pi'_\theta(y \mid a', v, x^v)$, and $q_{\text{sens}}(y) \triangleq \pi'_\theta(y \mid a, v', x^v)$. We also assume that q_{inv} and q_{sens} are treated as fixed target distributions within a single optimization step (that is, they do not depend on the parameters with respect to which we differentiate) as described in Sec. 4.1.

With these assumptions, and suppressing the conditioning variables (a, v, x^v) for brevity, the per- (a, v, x^v) objective can be written as,

$$\mathcal{J}(p_\theta) = \sum_y p_\theta(y) r(y) - \beta \mathbb{D}_{\text{KL}}(p_\theta \parallel p_{\text{ref}}) - \beta_{\text{inv}} \mathbb{D}_{\text{KL}}(p_\theta \parallel q_{\text{inv}}) + \beta_{\text{sens}} \mathbb{D}_{\text{KL}}(p_\theta \parallel q_{\text{sens}}), \quad (13)$$

subject to $p_\theta(y) \geq 0$ and $\sum_y p_\theta(y) = 1$. We can find the optimal policy that maximizes Eq. (13) using Lagrange’s method. We introduce a Lagrange multiplier λ for the normalization constraint, and expand the KL divergence terms to obtain,

$$\begin{aligned} \mathcal{J}'(p_\theta, \lambda) = & \sum_y p_\theta(y) r(y) - \beta \sum_y p_\theta(y) \log \frac{p_\theta(y)}{p_{\text{ref}}(y)} - \beta_{\text{inv}} \sum_y p_\theta(y) \log \frac{p_\theta(y)}{q_{\text{inv}}(y)} \\ & + \beta_{\text{sens}} \sum_y p_\theta(y) \log \frac{p_\theta(y)}{q_{\text{sens}}(y)} + \lambda \left(\sum_y p_\theta(y) - 1 \right). \end{aligned} \quad (14)$$

To obtain the stationary condition, we take the partial derivative of \mathcal{J}' with respect to $p_\theta(y)$ and set it to zero,

$$\begin{aligned} 0 = \frac{\partial \mathcal{L}}{\partial p_\theta(y)} = & r(y) - \beta \left(\log p_\theta(y) - \log p_{\text{ref}}(y) + 1 \right) - \beta_{\text{inv}} \left(\log p_\theta(y) - \log q_{\text{inv}}(y) + 1 \right) \\ & + \beta_{\text{sens}} \left(\log p_\theta(y) - \log q_{\text{sens}}(y) + 1 \right) + \lambda. \end{aligned} \quad (15)$$

We can now group the terms by $\log p_\theta(y)$ and collect the constants. Additionally, we define $\tau \triangleq \beta + \beta_{\text{inv}} + \beta_{\text{sens}}$ for simplicity. Then Eq. (15) becomes,

$$0 = r(y) - \tau \log p_\theta(y) + \beta \log p_{\text{ref}}(y) + \beta_{\text{inv}} \log q_{\text{inv}}(y) - \beta_{\text{sens}} \log q_{\text{sens}}(y) + (\lambda - \beta - \beta_{\text{inv}} + \beta_{\text{sens}}). \quad (16)$$

Finally, we can arrange the above equation to isolate $\log p_\theta(y)$ as,

$$\log p_\theta(y) = \frac{1}{\tau} \left(r(y) + \beta \log p_{\text{ref}}(y) + \beta_{\text{inv}} \log q_{\text{inv}}(y) - \beta_{\text{sens}} \log q_{\text{sens}}(y) \right) + C, \quad (17)$$

where the constant C absorbs $\lambda - \beta - \beta_{\text{inv}} + \beta_{\text{sens}}$ and enforces normalization.

Exponentiating Eq. (17) yields, up to a normalization constant,

$$p_\theta(y) \propto \exp(r(y)/\tau) p_{\text{ref}}(y)^{\beta/\tau} q_{\text{inv}}(y)^{\beta_{\text{inv}}/\tau} q_{\text{sens}}(y)^{-\beta_{\text{sens}}/\tau} \quad (18)$$

$$\implies \pi_\theta^*(y | a, v, x^v) \propto \exp(r(a, v, x^v, y)/\tau) \pi_{\text{ref}}(y | a, v, x^v)^{\beta/\tau} \pi'_\theta(y | a', v, x^v)^{\beta_{\text{inv}}/\tau} \pi'_\theta(y | a, v', x^v)^{-\beta_{\text{sens}}/\tau} \quad (19)$$

which is exactly Eq. (6).

A.2. Reward Function for Optimal Policy

Starting from Eq. (6), we take the natural logarithm of both sides and isolate $r(a, v, x^v, y)$. Absorbing the normalization constant into a function $W(a, v, x^v)$ that does not depend on y gives,

$$\begin{aligned} \tau \log \pi_\theta(y | a, v, x^v) &= r(a, v, x^v, y) + \beta \log \pi_{\text{ref}}(y | a, v, x^v) \\ &\quad + \beta_{\text{inv}} \log \pi'_\theta(y | a', v, x^v) - \beta_{\text{sens}} \log \pi'_\theta(y | a, v', x^v) + W(a, v, x^v), \end{aligned} \quad (20)$$

which, upon rearranging yields,

$$\begin{aligned} r(a, v, x^v, y) &= \tau \log \pi_\theta(y | a, v, x^v) - \beta \log \pi_{\text{ref}}(y | a, v, x^v) \\ &\quad - \beta_{\text{inv}} \log \pi'_\theta(y | a', v, x^v) + \beta_{\text{sens}} \log \pi'_\theta(y | a, v', x^v) + W(a, v, x^v), \end{aligned} \quad (21)$$

which is Eq. (7). The function $W(a, v, x^v)$ is determined by enforcing that $\sum_y \pi_\theta^*(y | a, v, x^v) = 1$ and does not affect optimization under pairwise preference models, since it cancels in likelihood ratios.

A.3. Decoupled Loss Function

For a given a triple $((a, v, x^v), y_w, y_l)$ and the reward $r(\cdot)$ in Eq. (7), the Bradley Terry model assigns the probability that y_w is preferred over y_l as

$$\Pr[y_w \succ y_l | a, v, x^v] = \sigma\left(r(a, v, x^v, y_w) - r(a, v, x^v, y_l)\right),$$

where $\sigma(t) = 1/(1 + e^{-t})$ is the sigmoid function. Using Eq. (7), the difference $r(a, v, x^v, y_w) - r(a, v, x^v, y_l)$ cancels the function $W(a, v, x^v)$ and yields

$$\begin{aligned} &\tau \left(\log \pi_\theta(y_w | a, v, x^v) - \log \pi_\theta(y_l | a, v, x^v) \right) - \beta \left(\log \pi_{\text{ref}}(y_w | a, v, x^v) - \log \pi_{\text{ref}}(y_l | a, v, x^v) \right) \\ &\quad - \beta_{\text{inv}} \left(\log \pi'_\theta(y_w | a', v, x^v) - \log \pi'_\theta(y_l | a', v, x^v) \right) + \beta_{\text{sens}} \left(\log \pi'_\theta(y_w | a, v', x^v) - \log \pi'_\theta(y_l | a, v', x^v) \right). \end{aligned} \quad (22)$$

Taking the negative expected log-likelihood over the preference dataset $\mathcal{D}_{\text{text}}^{\text{pref}}$ yields Eq. (8).

A.4. Symmetric Objective for Audio-Related Prompts

For prompts x^a that are related to the audio modality, the roles of audio and visual inputs are exchanged. The objective in Eq. (5) becomes,

$$\begin{aligned} \max_{\pi_\theta} \mathbb{E} \left[r(a, v, x^a, y) \right] &- \beta \mathbb{D}_{\text{KL}}\left(\pi_\theta(\cdot | a, v, x^a) \parallel \pi_{\text{ref}}(\cdot | a, v, x^a)\right) \\ &- \beta_{\text{inv}} \mathbb{D}_{\text{KL}}\left(\pi_\theta(\cdot | a, v, x^a) \parallel \pi_\theta(\cdot | a, v', x^a)\right) \\ &+ \beta_{\text{sens}} \mathbb{D}_{\text{KL}}\left(\pi_\theta(\cdot | a, v, x^a) \parallel \pi_\theta(\cdot | a', v, x^a)\right), \end{aligned} \quad (23)$$

Table 7. Training compute for baselines and MoD-DPO variants.

| Method | Data Preproc. (Offline) | Per Training Iteration | | | | Total till Train. Converg. | | |
|------------|-------------------------|------------------------|--------------------|--------------|--------------------|----------------------------|---------|---|
| | | # Fwd. | | # Back. | | # hrs | # iters | FLOPS _↓ ($\times 10^{18}$) |
| | | π_θ | π_{ref} | π_θ | π_{ref} | | | |
| Vanila DPO | - | 2 | 2 | 2 | 0 | 4.3 | 5k | 13.75 |
| OmniDPO | a', v' | 4 | 4 | 4 | 0 | 3.0 | 3k | 16.53 |
| MoD-DPO | a', v' | 6 | 2 | 2 | 0 | 2.0 | 1.8k | 7.43 |
| MoD-DPO++ | a', v' | 6 | 4 | 2 | 0 | 1.8 | 1.5k | 7.23 |

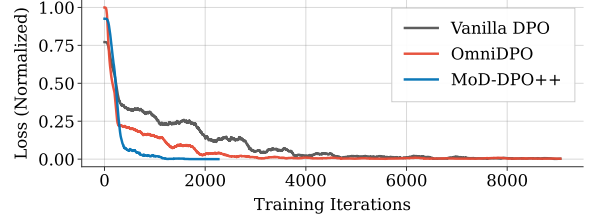


Figure 8. Training loss of baselines and MoD-DPO++.

where invariance now penalizes deviations when the irrelevant modality (visual) is corrupted and sensitivity rewards deviations when the relevant modality (audio) is corrupted. Repeating the derivations in Supp. A.1 and Supp. A.2 with a and v exchanged yields the audio counterpart of Eq. (8):

$$\begin{aligned} \mathcal{L}_{\text{MoD}}^a = -\mathbb{E} \left[\log \sigma \left(\tau \log \frac{\pi_\theta(y_w | a, v, x^a)}{\pi_\theta(y_l | a, v, x^a)} - \beta \log \frac{\pi_{\text{ref}}(y_w | a, v, x^a)}{\pi_{\text{ref}}(y_l | a, v, x^a)} \right. \right. \\ \left. \left. - \beta_{\text{inv}} \log \frac{\pi'_\theta(y_w | a, v', x^a)}{\pi'_\theta(y_l | a, v', x^a)} + \beta_{\text{sens}} \log \frac{\pi'_\theta(y_w | a', v, x^a)}{\pi'_\theta(y_l | a', v, x^a)} \right) \right]. \end{aligned} \quad (24)$$

Consequently, the final loss $\mathcal{L}_{\text{MoD}} = \mathcal{L}_{\text{MoD}}^v + \mathcal{L}_{\text{MoD}}^a$ in Eq. (9) follows.

A.5. (Optional) Objective for Prompts requiring both audio and visual information

For prompts x^{av} that require both audio and visual information for responding, we drop the *invariance* term in Eq. (5). The objective in Eq. (5) becomes,

$$\begin{aligned} \max_{\pi_\theta} \mathbb{E} \left[r(a, v, x^{av}, y) \right] - \beta \mathbb{D}_{\text{KL}} \left(\pi_\theta(\cdot | a, v, x^{av}) \parallel \pi_{\text{ref}}(\cdot | a, v, x^{av}) \right) \\ + \beta_{\text{sens}} \mathbb{D}_{\text{KL}} \left(\pi_\theta(\cdot | a, v, x^{av}) \parallel \pi_\theta(\cdot | a', v', x^{av}) \right), \end{aligned} \quad (25)$$

and the corresponding loss function for audiovisual prompts becomes the following,

$$\begin{aligned} \mathcal{L}_{\text{MoD}}^{av} = -\mathbb{E} \left[\log \sigma \left(\tau \log \frac{\pi_\theta(y_w | a, v, x^{av})}{\pi_\theta(y_l | a, v, x^{av})} - \beta \log \frac{\pi_{\text{ref}}(y_w | a, v, x^{av})}{\pi_{\text{ref}}(y_l | a, v, x^{av})} \right. \right. \\ \left. \left. + \beta_{\text{sens}} \log \frac{\pi'_\theta(y_w | a', v', x^{av})}{\pi'_\theta(y_l | a', v', x^{av})} \right) \right]. \end{aligned} \quad (26)$$

A.6. Training compute details

We report the detailed compute comparison of MoD-DPO with Vanilla DPO [31] and OmniDPO [4] in Tab. 7. As noted in Sec. 4.2, MoD-DPO++ adds forward passes through the policy model π_θ . Compared to OmniDPO, it uses the same data augmentation (hence same data processing compute) but two extra forward passes for policy π_θ and reference π_{ref} (see Tab. 7). For MoD-DPO++, since π'_θ in Eq. (6) is treated as fixed (see Sec. 4.1), no gradients are required, resulting in fewer backward passes and lower FLOPs per iteration. As shown in Fig. 8 and Tab. 7, MoD-DPO++ converges nearly twice as fast as OmniDPO, and all models are trained to convergence.

B. Preference Data Details

B.1. Detailed Pipeline

B.1.1. Stage - 1

We use the prompts present in Fig. 10 to obtain audio prompts from AudioFlamingo 3 [12] and the visual prompts from GPT-4o [18]. For audio captioning, we pass the entire audio to the AudioFlamingo 3 model and for visual captioning, we pass frames at a frame rate of 1 frame per second to GPT-4o for visual captioning. Additionally, we use RAM++ [17] to obtain the visual tags present in the video by passing frames from the video at 1 FPS to the RAM++ model, and we take a union of all the tags obtained as the objects/events present in the video.

Table 8. Examples from the generated preference dataset.

| Audiovisual Input | Prompt x | Chosen Response y_w | Rejected Response y_l |
|---|---|---|--|
|  <p>Audio: "(machine whirring...)"</p> | Is the sewing machine visible in the video? | Yes, the object is visible in the video. The video captures a close-up view of an embroidery machine in action, stitching a logo onto a cap. | No, the object is not visible in the video. We can only hear the sound of a machine operating with some noise. |
|  <p>Audio: "(dog panting...)"</p> | Is the chair making sound in the audio? | No, the object is not making a sound in the audio. The audio indicates that the primary sound is panting, likely from a dog, and there is no sound coming from a chair. | Yes, the object is making a sound in the audio. The dog can be seen barking on the noisy chair. |

B.1.2. Stage - 2

For the captioning task, Stage-2 involves associating the prompts “Describe only the audio in detail.” and “Describe only the video in detail.” to the audio and visual captions obtained in Stage-1, respectively. For the object/event presence subtask, there are three sub-stages involved.

First, we pass the audio and visual information obtained in the form of audio/visual captions and video tags to GPT-4o using prompts in Fig. 11 and classify different objects/events present in the inputs to the following categories – “in-view sound source”, “in-view sound”, “in-view silent object”, “out-of-view sound source”, and “out-of-view sound”. This classification is similar to that of AVHBench [35] and simplifies the automatic generation of QA pairs.

Next, we automatically generate the QA pairs using the following template – “Is the {object/event} making sound in the audio?” for audio presence (*video-driven audio hallucination*) tasks and “Is the {object/event} visible in the video?” for visual presence (*audio-driven visual hallucination*) tasks. For the visual presence tasks, objects/events classified as “in-view sound source” are assigned an answer of “Yes”, and “out-of-view sound source” & “out-of-view sounds” are assigned an answer of “No”. For the audio presence tasks, objects/events classified as “in-view sound source” & “in-view sound” are assigned an answer of “Yes” and “in-view silent objects” are assigned an answer of “No”.

Finally, since the data generation pipeline in the above paragraph is automatic, we run a round of automatic verification through GPT-4o using prompts in Fig. 12 to ensure that the generated data are indeed consistent and correct.

B.1.3. Stage - 3

As described in Sec. 4.3, we generate the preference dataset using GPT-4o by using the information present in the other modality to construct the rejected responses. Figs. 13 and 14 shows the prompts used for the generation of preference data for the captioning task and object/event presence tasks, respectively.

B.2. Preference Data Samples

Tab. 8 shows some examples from the generated preference dataset.

C. Experimental Details

C.1. Evaluation Metrics

For evaluation on AVHBench [35], we use the following metrics:

- *Precision*: Percent of samples which are correctly predicted among the samples which have the ground truth answer as “Yes”.
- *Recall*: Percent of samples which are correctly predicted among the samples which have the ground truth answer as “No”.
- *Accuracy*: Overall number of samples correctly predicted.

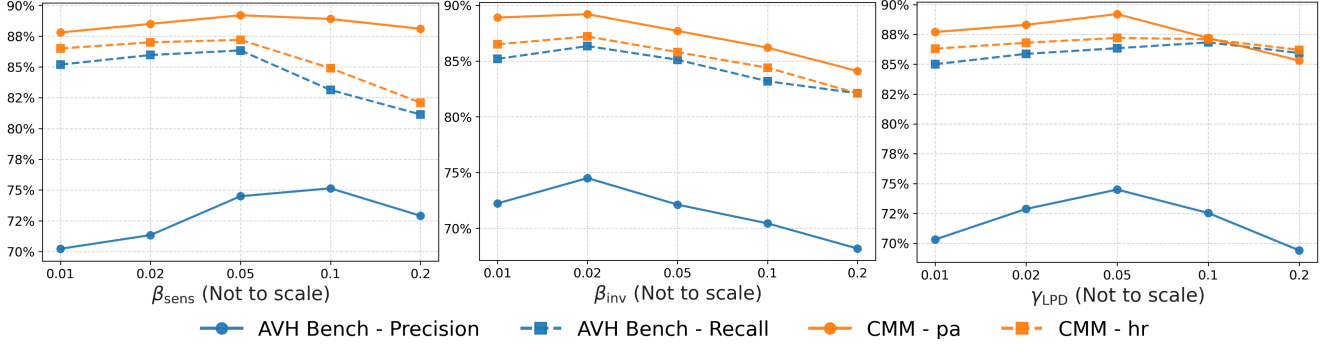


Figure 9. Effect of varying different hyperparameters involved in MoD-DPO. Default values: $\beta_{\text{sens}} = 0.05$, $\beta_{\text{inv}} = 0.02$, $\gamma_{\text{LPD}} = 0.05$. When varying one hyperparameter, others are set to their default values.

Table 9. Comparison with decode-time approaches.

| Method | AVHBench [35] | | | CMM [25] | |
|--------------------|---------------|--------------|--------------|-------------|-------------|
| | Acc. | Pre. | Rec. | pa | hr |
| Qwen 2.5 Omni [43] | 72.07 | 60.50 | 83.65 | 86.4 | 84.6 |
| + VCD* [21] | 74.74 | 61.64 | 87.84 | 86.9 | 85.2 |
| + AVCD [21] | 75.57 | 62.85 | 88.28 | 87.2 | 85.6 |
| + MoD-DPO++ | 80.42 | 74.50 | 86.34 | 89.2 | 87.2 |

- *F1 Score*: Harmonic mean of Precision and Recall.

For evaluation on Curse of Multi-Modalities [25], we use the following metrics:

- *Perception Accuracy (pa)*: Percent of samples which are correctly predicted among the samples which have the ground truth answer as “Yes”.
- *Hallucination Resistance (hr)*: Percent of samples which are correctly predicted among the samples which have the ground truth answer as “No”.

For evaluation on general benchmarks – DailyOmni [58], MVBench [26], and MMAU [33] – we use the average accuracy over different subtasks of the benchmark.

C.2. Evaluation Protocol

For “Yes”/“No” tasks present in AVHBench and CMM, we parse the model responses using string matching to obtain the result. For multiple-choice tasks in general benchmarks, we use regex to parse the model responses and get the predicted choice.

C.3. Baseline Implementations

We compare MoD-DPO and MoD-DPO++ with naive DPO [31] and OmniDPO [4]. We use our generated preference data from Sec. 4.3 to train both the preference optimization baselines. Additionally, we also compare with other state-of-the-art omni LLMs, including VideoLLaMA 2 [8] (7B params), VITA-1.5 [10] (7B params), Qwen 3 Omni [44] (35B params), and OmniVinci [47] (9B params). For all the omni LLM baselines, we use their official codebase and use default parameters for inference.

D. Additional Results

D.1. Hyper-parameter Tuning

As described in Sec. 6.2, Fig. 9 shows how different hyperparameter values affect the performance of the proposed approach on different benchmarks. Please refer to Sec. 6.2 (**Strength of hyperparameters**) for a detailed explanation.

D.2. Comparison with decode-time approaches

Tab. 9 shows comparison with decode-time approaches AVCD [21] and VCD* (default settings used from [21]). These decode-time approaches result in moderate gains over the reference model, whereas MoD-DPO++ gains are superior.

D.3. Multi-turn omni-modal results

To show the performance improvement on multi-turn dialog scenarios, we perform evaluation on the audiovisual task subset of OmniDialog benchmark [32] and report results in Tab. 10. We can observe that both MoD-DPO and MoD-DPO++ result in a performance improvement over the baseline, however the improvement in the case of MoD-DPO++ is more pronounced. Moreover, MoD-DPO++ results in a superior performance compared to OmniDPO [4].

Table 10. OmniDialog Results

| Method | OmniDialog |
|---------------|--------------|
| Qwen 2.5 Omni | 83.91 |
| + OmniDPO | 84.18 |
| + MoD-DPO | 83.96 |
| + MoD-DPO++ | 85.86 |

E. Prompt Pool

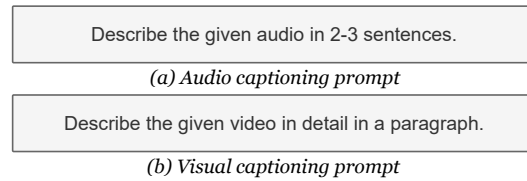


Figure 10. **Audio and visual captioning prompts** used in Stage-1 of Preference Data Generation Sec. 4.3. Audio captions are obtained from AudioFlamingo 3 [12] and visual captions are obtained from GPT-4o [18].

```
""The "caption" provides the explanation about audio event. The "visual tagging" identifies the observable visual objects or actions.
If similar objects from the "caption" are found in the "visual tagging", it is assumed to exist in-view. If not, it is assumed to exist out-of-view.
The "information" aims to summarize the inferable audio and visual information:
- In-view sound source is the object that makes sound and is visible in the scene,
- In-view sound is the type of sound that the object in the scene makes,
- In-view silent object is the object that does not make sound but is visible in the scene,
- Out-of-view sound source is the expected object that makes sound and is not visible in the scene, and
- Out-of-view sound is the type of sound that the object out of the scene makes.

You are required to classify and return the objects into the above categories for the given caption and visual tagging.

Following are a few examples:
===== Example 1 =====
Caption: In the room, a woman held a can of stuff in her hand and showed it back and forth. The sound of xylophone and children's music came from the background music.
Visual Tagging: beverage | green | squeeze | food | orange juice | market | shopping cart | catch | red | fill | shopping basket | play | cart | bin | basket | can | woman | hand | push |
produce | container | bottle | juice
-----
In View Sound Source: []
In View Sound: []
In View Silent Object: [beverage, food, orange juice, shopping cart, shopping basket, cart, bin, basket, hand, container, bottle, juice]
Out of View Sound Source: ["xylophone", "children"]
Out of View Sound: ["xylophone music", "children's music"]
===== Example 2 =====
Caption: With the sound of chewing, a red bike was parked outside, and a man in a dark top stood looking at the bike.
Visual Tagging: motorbike | red | motorcycle | lean | hose | man | pavement | brown | moped | floor | park | lock | attach | walk | night | person | tire | curb | stand | pole | bicycle
-----
In View Sound Source: []
In View Sound: []
In View Silent Object: [motorbike, motorcycle, pavement, moped, floor, park, lock, tire, curb, pole, bicycle]
Out of View Sound Source: ["man"]
Out of View Sound: ["chewing"]
=====

Now provide the classification for the following:

Caption: "" + REPLACE AUDIO CAPTION STRING + ""
Visual Tagging: "" + REPLACE VIDEO TAGS STRING + ""

Return the "information" in the following JSON format:
{
  "in_view_sound_source": [list of strings],
  "in_view_sound": [list of strings],
  "in_view_silent_object": [list of strings],
  "out_of_view_sound_source": [list of strings],
  "out_of_view_sound": [list of strings]
}""
```

Figure 11. **QA Generation Prompt - Stage 2.1.** used for classifying the events/objects in the current audiovisual input into different classes similar to AVHBench [35].

""You will be given with a audio-related question and an answer for a given audiovisual input. Additionally, you will also have access to the audio caption for the input.

- Your task is to verify whether the answer is correct for the question.
- The question is about whether a specific object/event is audible in the audio or not.

Return your response in the following JSON format:

```
{
  "verdict": "Yes" or "No" or "Question Invalid",
  "explanation": "brief explanation justifying your verdict based on the audio caption"
}
```

=====

Audio Caption: "" + REPLACE_AUDIO_CAPTION_STRING + ""

Question: "" + REPLACE_QUESTION_STRING + ""

Answer: "" + REPLACE_ANSWER_STRING

(a) Video-driven Audio Hallucination

""You will be given with a vision-related question and an answer for a given audiovisual input. Additionally, you will also have access to the visual caption for the input.

Your task is to generate two sets of detailed answers for the given question.

- First, should start with the given answer (yes/no) and then justify it based on the provided visual caption.
- Second, should be opposite to the given answer (no/yes) and then provide a random reason to justify it.

Return your response in the following JSON format:

```
{
  "chosen": "detailed answer starting with the given answer",
  "rejected": "detailed answer starting with the opposite of the given answer"
}
```

=====

Visual Caption: "" + REPLACE_VIDEO_CAPTION_STRING + ""

Question: "" + REPLACE_QUESTION_STRING + ""

Answer: "" + REPLACE_ANSWER_STRING

(a) Audio-driven Video Hallucination

Figure 12. **QA Generation Verification Prompt - Stage 2.3.** used to verify the automatic QAs generated for video-driven audio hallucination and audio-driven video hallucination.

""You will be provided with a visual and audio information for a given video. Visual information includes a video caption and a set of tags associated with the video, while audio information includes an audio caption.

Based on this information, you need to generate two sets of captions ONLY ABOUT THE AUDITORY INFORMATION as per the following requirements:

1. Correct caption: Generate an accurate caption that describes the content of the audio based on the provided AUDIO caption.
2. Inconsistent caption (video-relevant): This should follow the same tone and style as the correct caption but should include WRONG information about AUDITORY entities in the audio, based on the VIDEO CAPTION and TAGS.

Frame your responses in a way that they answer to the following question: "Describe only what you hear?". Do not say anything about the visual or video content in the generated captions. Only describe the audio content and respond based on the above two criterias.

Return your response in the following JSON format: {"chosen": "correct caption here", "rele_reject_1": "inconsistent caption (video-relevant)"}

=====

Video Caption: "" + REPLACE VIDEO CAPTION STRING + ""\n

Video Tags: "" + REPLACE VIDEO TAGS STRING + ""\n

Audio Caption: "" + REPLACE AUDIO CAPTION STRING + ""\n

""

(a) Audio Captioning

You will be provided with a visual and audio information for a given video. Visual information includes a video caption and a set of tags associated with the video, while audio information includes an audio caption.

Based on this information, you need to generate two sets of captions ONLY ABOUT THE VISUAL INFORMATION as per the following requirements:

1. Correct caption: Generate an accurate caption that describes the content of the video based on the provided video caption and tags.
2. Inconsistent caption (audio-relevant): This should follow the same tone and style as the correct caption but should include WRONG information about VISUAL entities in the video, based on the AUDIO CAPTION.

Frame your responses in a way that they answer to the following question: "Describe only what you see?". Do not say anything about the audio content in the generated captions. Only describe the visual content and respond based on the above three criterias.

Return your response in the following JSON format: {"chosen": "correct caption here", "rele_reject_1": "inconsistent caption (audio-relevant)"}

=====

Video Caption: "" + REPLACE VIDEO CAPTION STRING + ""\n

Video Tags: "" + REPLACE VIDEO TAGS STRING + ""\n

Audio Caption: "" + REPLACE AUDIO CAPTION STRING + ""\n

""

(b) Visual Captioning

Figure 13. **Preference Data Generation Prompt - Stage 3 (Captioning)** used to generate preference data pairs for the captioning task for training MoD-DPO.

""You will be given with a audio-related question and an answer for a given audiovisual input. Additionally, you will also have access to the audio caption for the input. Your task is to generate two sets of detailed answers for the given question.

- First, should start with the given answer (yes/no) and then justify it based on the provided audio caption.
- Second, should be opposite to the given answer (no/yes) and then provide a reason related on the given VISUAL CAPTION to justify it.

Return your response in the following JSON format:

```
{
  "chosen": "detailed answer starting with the given answer",
  "rejected": "detailed answer starting with the opposite of the given answer"
}
```

=====

Audio Caption: "" + REPLACE AUDIO CAPTION STRING + ""

Visual Caption: "" + REPLACE VIDEO CAPTION STRING + ""

Question: "" + REPLACE QUESTION STRING + ""

Answer: "" + REPLACE ANSWER STRING

(a) Video-driven Audio Hallucination

""You will be given with a vision-related question and an answer for a given audiovisual input. Additionally, you will also have access to the visual caption and audio caption for the input. Your task is to generate two sets of detailed answers for the given question.

- First, should start with the given answer (yes/no) and then justify it based on the provided visual caption.
- Second, should be opposite to the given answer (no/yes) and then provide a reason related on the given AUDIO CAPTION to justify it.

Return your response in the following JSON format:

```
{
  "chosen": "detailed answer starting with the given answer",
  "rejected": "detailed answer starting with the opposite of the given answer"
}
```

=====

Visual Caption: "" + REPLACE VIDEO CAPTION STRING + ""

Audio Caption: "" + REPLACE AUDIO CAPTION STRING + ""

Question: "" + REPLACE QUESTION STRING + ""

Answer: "" + REPLACE ANSWER STRING

(b) Audio-driven Video Hallucination

Figure 14. **Preference Data Generation Prompt - Stage 3 (Presence)** used to generate preference data pairs for the object/event presence task for training MoD-DPO.